ISSN 1063-7834, Physics of the Solid State, 2008, Vol. 50, No. 12, pp. 2289–2294. © Pleiades Publishing, Ltd., 2008.
Original Russian Text © I.S. Édelman, O.S. Ivanova, K.P. Polyakova, V.V. Polyakov, O.A. Bayukov, 2008, published in Fizika Tverdogo Tela, 2008, Vol. 50, No. 12, pp. 2192–2197.

MAGNETISM AND FERROELECTRICITY

Evolution of the Structure and Magneto-Optical Properties of $Mn_xFe_{3-x}O_4$ Films Prepared by Solid-State Reactions

I. S. Édelman[a], O. S. Ivanova[b], K. P. Polyakova[a], V. V. Polyakov[a], and O. A. Bayukov[a]

[a] *Kirensky Institute of Physics, Siberian Branch, Russian Academy of Sciences, Akademgorodok, Krasnoyarsk, 660036 Russia*
e-mail: ise@iph.krasn.ru

[b] *Siberian Federal University, Svobodny pr. 79, Krasnoyarsk, 660041 Russia*

Received April 7, 2008

Abstract—This paper reports on the results of investigations into the structure and the magnetic and magneto-optical properties of thin films $Mn_xFe_{3-x}O_4$ prepared by solid-state reactions: isothermal annealing, self-propagating high-temperature synthesis, and a combination of these two regimes. The regimes favorable for the formation of films close in composition and structure to the stoichiometric compounds $MnFe_2O_4$ or Fe_3O_4 are established. The features observed in the spectral response of the magneto-optical Faraday effect and of the magnetic circular dichroism of the $MnFe_2O_4$ films are considered in terms of the electronic transitions in magnetic ions, primarily Fe^{3+}, which occupy octahedral positions in the spinel structure.

PACS numbers: 78.20.Ls, 68.55.Ln

DOI: 10.1134/S106378340812010X

1. INTRODUCTION

Spinel ferrites of the general formula MFe_2O_4, where M stands for a divalent cation, form a class of magnetic oxides which both have application potential and are of interest from the standpoint of basic science. Their representatives, magnetite Fe_3O_4 and manganese ferrite $MnFe_2O_4$, have attracted the particular attention. Magnetite is used in dye industry as precursor in production of magnetic liquids, as a heterogeneous catalyst, etc. Manganese ferrite is a basic material of microwave technology. Spinel ferrites occupy also a unique place in the development of magneto-optical devices intended for operation in the wavelength range 0.8–1.5 μm because of their high transparency and large Faraday rotation coefficient. The magneto-optical properties of oxide spinels depend not only on their chemical composition but on the distribution of magnetic cations over the crystallographic positions in the spinel lattice as well, and, hence, on the technology of their preparation. We report on a study of the magnetic and magneto-optical properties of polycrystalline $Mn_xFe_{3-x}O_4$ films in connection with the specific features of their structure. The films were prepared by solid-state reactions in three different regimes: isothermal annealing; self-propagating high-temperature synthesis (SHS) [1–3], which has become very popular recently; and their combination. The SHS technique had been first put to practical use in preparation of thin films of ferrites, more specifically, $Co_{0.4}CrFe_{1.6}O_4$ [4].

2. FILM PREPARATION AND EXPERIMENTAL TECHNIQUES

Polycrystalline Mn-ferrite films were produced in solid-state reactions initiated in metal/oxide layered structures. Solid-state reactions can proceed in the regimes of both isothermal annealing and SHS [4]. For SHS to set in, the original mixture has to contain fuel and oxidizer to maintain burning. In oxide synthesis, it is, as a rule, the metal that serves as fuel. The oxidizer is oxygen. Oxidation of the metal is the main reaction, because it is this process that provides the liberation of heat necessary for supporting the SHS. Two sources of oxygen, internal and external, can be used.

The films of manganese ferrite were produced by the following solid-phase reaction

$$2MnO + 2Fe + 3O_2 = 2MnFe_2O_4.$$

The reagents are arranged as layers in the MnO/Fe film structure.

The Mn films were deposited by thermal evaporation in vacuum at a base pressure $P = 10^{-5}$ Torr on a substrate (cover glass) maintained at 450–500 K. Deposition was effected in several evaporation cycles performed under identical conditions. Samples **1**–**4** were prepared simultaneously in one deposition cycle. After this, the Mn films were oxidized for 1 h in air at a temperature of 650 K.

Atop the oxidized Mn films, the Fe layer was deposited by thermal evaporation in the conditions described above. The thickness of each layer varied from 30 to

Table 1. Composition of the final phase and film thickness from x-ray fluorescence data

Sample	Structure	Thickness, nm	Solid-state reaction conditions	M_S, G
1	Predominantly Fe_3O_4	190	SHS (~700 K)	450
2	Predominantly Mn ferrite	190	Isothermal annealing at 620 K, 3 h	250–350
3	Predominantly Mn ferrite	190	Isothermal annealing at 720 K, 3 h	150
4	Predominantly Mn ferrite	190	SHS + isothermal annealing at 770 K, 10 min	
5	$Mn_{1.2}Fe_{1.8}O_4$	130	Isothermal annealing at 620 K, 3 h	320
6	Predominantly Fe_3O_4 (with ^{57}Fe)	450	SHS + isothermal annealing at 700 K, 6 h	450
7	$MnFe_2O_4$ (with ^{57}Fe)	230	SHS + isothermal annealing at 620 K, 3 h	150

70 nm. In two cases, 50% of the Fe charge was the ^{57}Fe isotope. The MnO/Fe bilayer samples thus prepared were subjected to thermal treatment in the solid-state reaction regime. Three different techniques were employed, namely, SHS, isothermal annealing, and SHS followed by isothermal annealing.

To prepare ferrite films by SHS, the film structure was placed on a heater and heated with a rate of not less than 20 K/s (thermal explosion) to the temperature at which the SHS wave was initiated (~700 K). The wavefront propagation was readily visualized and was typical of thin film SHS [2].

The solid-state reaction under isothermal annealing was performed by heating in a furnace at temperatures of 620–720 K for 3 h. In the cases where annealing was performed after the SHS, it could differ in duration. The films prepared by solid-state reactions in layered structures had a smooth specular surface, irrespective of the actual solid-state reaction regime and annealing temperature. The 450-nm-thick films containing the ^{57}Fe iron isotope and prepared by SHS were an exclusion. These films were found to contain separate small (~0.5 mm^2) fragments which, being optically more dense, could be seen by eye in transmission. The synthesis conditions and the thickness of the samples are listed in Table 1.

The chemical composition of the samples (absolute content of Fe and Mn) was determined using the x-ray fluorescence analysis. Next the film thickness was estimated from x-ray diffraction measurements assuming the formula of the final reaction product. The x-ray diffraction patterns were recorded on a DRON-3 diffractometer (CuK_α radiation). The Mössbauer spectra were measured at room temperature with a $^{57}Co(Cr)$ source in the constant acceleration mode. The isomer chemical shifts are referenced to metallic iron α-Fe. The saturation magnetization was measured with a torsion magnetometer. The Faraday rotation was probed by modulating the light beam in the plane of polarization, with the angle of rotation measured to within ±0.2 min. The spectral interval covered was 450–1000 nm. The external magnetic field was 2 kOe. The magnetic circular dichroism (MCD), the difference in the absorption coefficients between waves that are right- and left-polarized with respect to the direction of magnetization of the material in which they propagate, was studied by modulating the light beam in phase [5]. The relative accuracy of measurements was not worse than ±0.5% of the measured value.

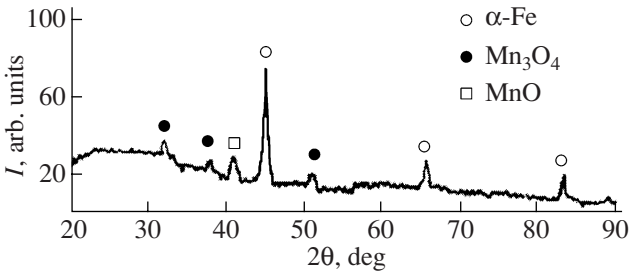

Fig. 1. X-ray diffraction pattern of the bilayer film (corresponding to sample **2**) before initiation of the solid-state reaction.

3. RESULTS

3.1. Structural and Phase Analysis

Figure 1 presents the x-ray diffraction pattern of a bilayer sample of manganese oxide with an iron layer deposited on top which was obtained before initiation of the solid-state reaction. The x-ray diffraction pattern is seen to contain the peaks corresponding to the α-Fe phase, Mn_3O_4, and MnO. Thus, the bilayer structure represents actually a superposition of a mixture of iron with the Mn_3O_4 and MnO oxides. The x-ray diffraction pattern of this film measured after the completion of the solid-state reaction run in the isothermal annealing regime at 620 K (Fig. 2) contains two reflections belonging to the $MnFe_2O_4$ ferrite phase. Tabulated data identify them as the strongest diffraction bands corresponding to the [311] and [400] interplanar distances [6]. The weak reflections could be assigned to either an iron oxide (α- and γ-Fe_2O_3) as an impurity phase or a surface film which forms as the sample cools down following isothermal annealing, a feature observed fre-

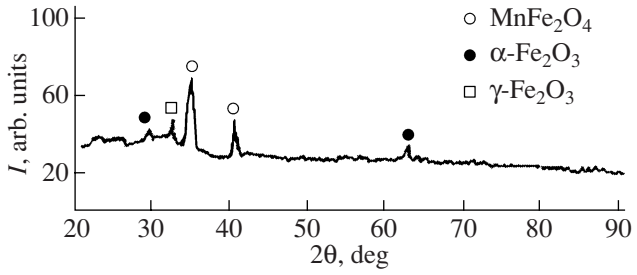

Fig. 2. X-ray diffraction pattern of sample **2**.

quently in the course of synthesis and thermal treatment of bulk ferrites and ferrite films. Samples **2–5** and **7** reveal a similar x-ray diffraction pattern. Thus, the x-ray diffraction patterns of film structures obtained after the completion of the solid-state reaction in the isothermal annealing regime suggest formation of polycrystalline manganese ferrite.

Figure 3a presents the Mössbauer spectrum of sample **7**. Note that the film that was subjected to the SHS reaction contains separate small (0.5 mm^2) regions of black color, presumably of the Fe_3O_4 residual phase, which disappear after annealing in air for 3 h. Table 2 lists the parameters of the hyperfine structure of the spectrum of sample **7**. This sample reveals iron positions whose Mössbauer parameters and, hence, the local environment are close to those in α-Fe_2O_3 hematite (~20%) and γ-Fe_2O_3 maghemite (~8%) [7]. The positions of the remaining iron (~78%) are close in parameters to those in manganese ferrite [8]. The higher values of the isomer chemical shifts and the large linewidths evidence the manganese ferrite to be nonstoichiometric. Just as the manganese ferrite, the maghemite has spinel structure $(Fe)[Fe_{5/3}\square_{1/3}]O_4$, where $\square$ stands for the cation vacancy. Thus, the spinel phase of sample **7** may be considered both as a solid solution γ-Fe_2O_3 + $MnFe_2O_4$ and as the manganese ferrite with cation vacancies.

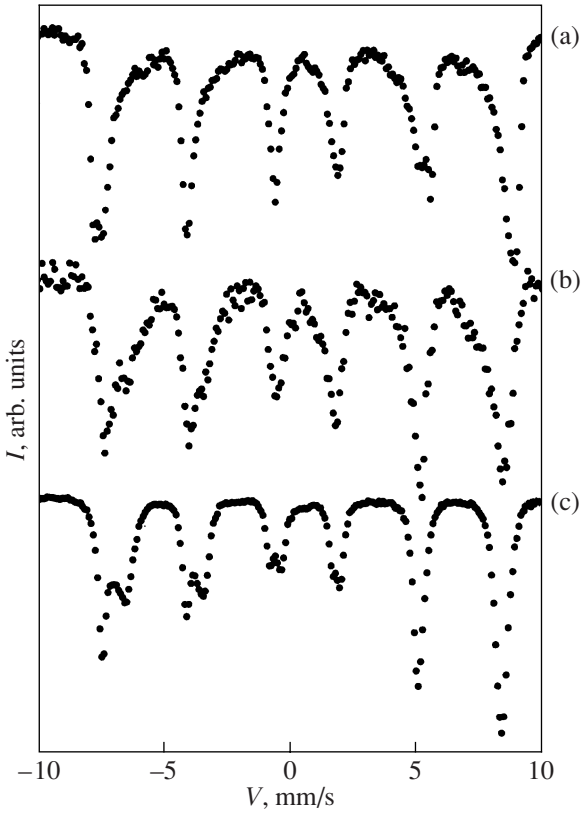

Fig. 3. Mössbauer spectra of samples (a) **7**, (b) **6**, and (c) natural magnetite.

A different pattern is observed for the thicker sample **6** (Fig. 3b) which reveals the presence of mixed-valence iron characteristic of the Fe_3O_4 magnetite. In Fig. 3c the response is compared with the spectrum of natural magnetite. Rough estimates performed by fit-

Table 2. Hyperfine structure parameters of the Mössbauer spectra (*IS* is the isomer chemical shift relative to α-Fe, *H* is the hyperfine field at iron nucleus, *QS* is the quadrupole splitting, *W* is the absorption line width, and *S* is the fractional occupancy of the inequivalent position)

Sample	*IS*, ±0.02 mm/s	*H*, ±5 kOe	*QS*, ±0.03 mm/s	*W*, ±0.03 mm/s	*S*, ±0.03	Structure
7	0.38	516	–0.32	0.27	0.21	α-Fe_2O_3
	0.33	501	0.43	0.26	0.08	γ-Fe_2O_3
	0.43	491	0	0.63	0.43	$MnFe_2O_4$
	0.45	446	0.13	0.72	0.14	
	0.44	385	0	0.98	0.15	
6	0.33	493	0.03	0.51	0.35	Fe_3O_4
	0.62	448	0	0.67	0.24	
	0.41	475	–0.12	0.38	1.12	$MnFe_2O_4$
	0.44	407	0	1.25	0.26	
	1.03	0	0.48	0.48	0.03	Fe^{2+}

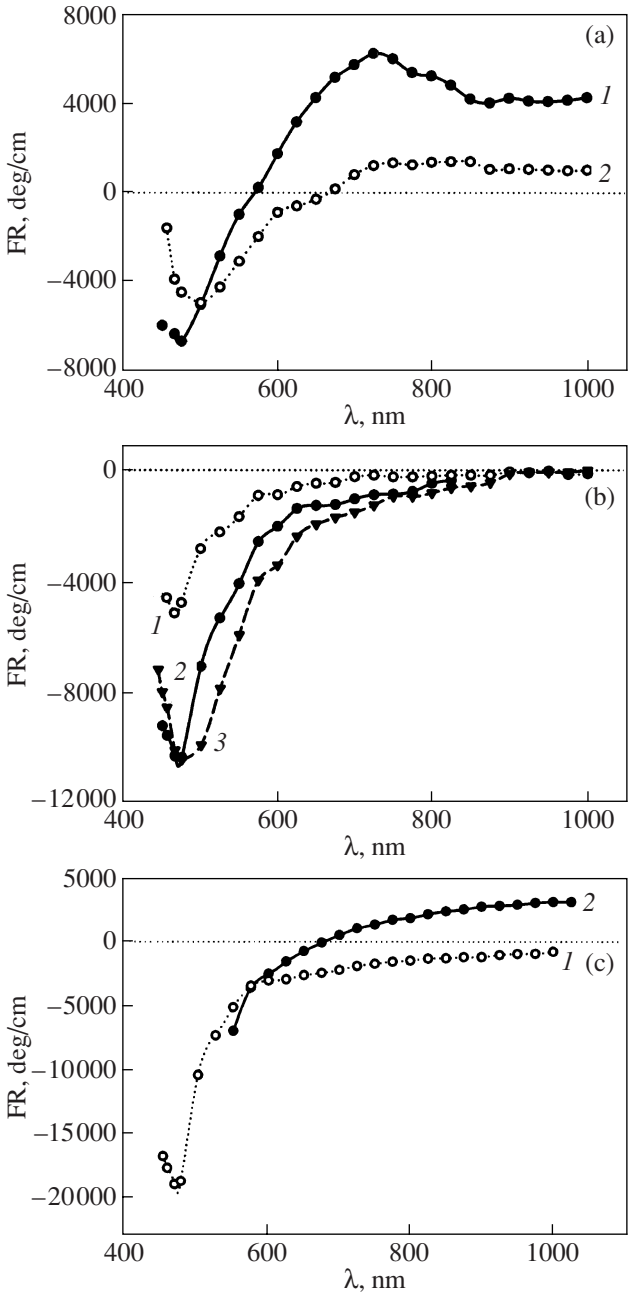

Fig. 4. Room-temperature FE spectral response measured in a magnetic field of 2 kOe for different samples (a) (*1*) **1** and (*2*) **4**; (b) (*1*) **3**, (*2*) **2**, and (*3*) **5**; and (c) (*1*) **6** and (*2*) **7**.

ting the experimental spectrum to four sextets and one doublet are listed in Table 2. We readily see that ~60% of the iron present in the film may reside in a local environment close to that in magnetite, and ~40%, to that in the manganese ferrite phase. Thus, sample **6** may represent actually a solid solution of magnetite and manganese ferrite. The presence in the reaction products of the above phases argues for the solid-state reaction not having been run to the end.

3.2. Magnetization

The results of magnetization measurements are listed in Table 1. The saturation magnetization M_S of the synthesized films is seen to depend on film thickness and the regimes of the solid-state reactions. In particular, the saturation magnetizations of the films prepared in the SHS solid-state reaction are substantially higher than those of the films obtained in a solid-state reaction performed under isothermal annealing. Because the principal kinetic parameter of these regimes is the reaction rate, the difference in the magnetizations may be due to different degrees of oxidation reached in the layered structures and, hence, to the presence of iron in a different valence state (Fe^{2+}) and, thus, of the magnetite as the impurity phase. This assumption is not at odds with the measurements of optical spectra of the films prepared in different solid-state reaction regimes.

The magnetizations of the films prepared by isothermal annealing at different temperatures are also seen to be different. The magnetization is observed to depend also on composition of the films prepared in the same conditions.

3.3. Magneto-Optical Effects

The spectral response of the Faraday effect (FE) is shown graphically in Fig. 4. The pattern of the FE spectrum in the long-wavelength region depends markedly on the solid-state reaction regime. Sample **1** prepared by SHS synthesis (without subsequent isothermal annealing) exhibits in the region of positive values a broad maximum centered about 700 mm (Fig. 4a, curve *1*). The presence of this maximum is a characteristic feature of the FE spectrum of Fe_3O_4 magnetite films [9]; it is assigned to the spin-allowed electronic transition in divalent iron ions. The presence of magnetite in this sample is evident both from the x-ray diffraction pattern (Fig. 1) and from the Mössbauer spectrum (Fig. 3). Thus, the oxidation reaction initiated by SHS does not come to the end. Subsequent annealing of this film at a temperature of 770 K for 10 min brings about a sharp decrease of this maximum (curve *2* in Fig. 4a), thus evidencing intensification of the process of oxidation of Fe^{2+} to Fe^{3+}. In the present case, however, this process does not reach completion. Isothermal annealing performed for a long time (without preliminary SHS) provides complete oxidation of the divalent Fe ions; the FE curves in the long-wavelength region obtained after such a treatment approach closely one another and do not contain any maxima (Fig. 4b). Prolonged annealing following SHS reaction brings about the same result (Fig. 4c, curve *1*). The effect of film thickness on the outcome of the solid-state reactions turned out unexpected results. The oxidation reaction in the sample of about twice larger thickness does not come to completion; indeed, a splitting characteristic of the magnetite appears in the Mössbauer spectrum, and

a long-wavelength positive maximum is seen again in the FE spectral response. One might think that the difference in the results of the solid-state reactions in the latter of the samples under discussion originates from the iron sample containing the ^{57}Fe isotope being of a different quality. However, the FE spectrum of a thinner sample, likewise with the isotope (sample **7**, table 1) coincides with those of samples **2**, **3**, and **5**. This suggests that the cross section of the solid-state reaction is smaller than the thickness of film **6**. By comparing the FE in the long-wavelength region in samples **1** and **6** one can estimate the cross section of the solid-state reaction, which is approximately 380 nm.

The FE spectra of all the samples studied reveal a negative maximum near the wavelength of 460 nm. This maximum is characteristic of Fe^{3+} ions in cubic environment [9–11]. It is assigned to the $^6A_{1g} \longrightarrow {}^4E_g, {}^4A_{1g}$ electronic transition taking place in Fe^{3+} ions in octahedral environment. This identification rests on the observation that this band is observed in iron borate which has only trivalent iron ions in octahedral positions. Manganese ions can also, however, contribute to the FE close to 460–500 nm. Interpretation of this region of the spectrum is made still more difficult by the possible contribution of Fe^{2+} ions, as this was found earlier (Fig. 2 in [9]). A comparison of FE and Mössbauer spectra (Fig. 3b) strongly suggests that sample **7** contains primarily one magnetic phase, $MnFe_2O_4$. The peak value of the FE at ~470 nm exceeds in this case substantially the corresponding values of FE in the other samples. One still cannot say much about the origin of such large differences among the FE effects in the short-wavelength maximum and the magnetizations measured on different samples, as well as about the absence of correlation between the magnitude of the FE and magnetization observed in some cases. A clear correlation between the FE features and magnetization is found to exist only for samples **2**, **3**, and **5** synthesized by isothermal annealing. This might stem from nonuniformities in samples forming in the SHS stage.

Now, we consider the MCD spectra, which in many cases offer more information than the FE response, because MCD is observed in narrow absorption bands. Figure 5 shows such a spectrum for sample **7**. At ≈450 nm (2.75 eV) one observes a strong maximum (of negative sign) which coincides in position with the one seen in the Kerr effect [12] in chemically prepared nanoparticles of the $Mn_{0.5}Fe_{2.5}O_4$ manganese ferrite. There is nothing strange in such a coincidence, because the MCD and the Kerr rotation originate primarily from the imaginary part of the nondiagonal component of the dielectric permittivity tensor of the material. Another distinct maximum (also of negative sign) is observed at ~660 nm. That the two features are of the same sign may indicate that they are associated with like ions on the same sublattice. Note that the iron borate $FeBO_3$, containing only trivalent iron ions in crystal positions of one type only, octahedral, revealed absorption bands at 435 and 610

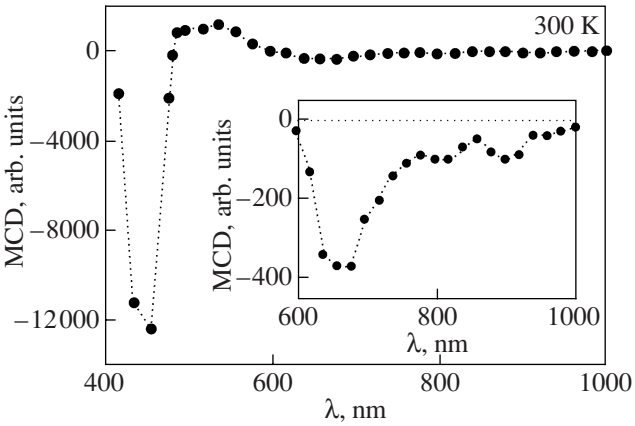

Fig. 5. MCD spectrum of sample **7**. The inset shows the long-wavelength region on an enlarged scale.

nm, which are produced by the $^6A_{1g} \longrightarrow {}^4E_g, {}^4A_{1g}$ and $^6A_{1g} \longrightarrow {}^4T_{2g}$ electronic transitions, accordingly [10, 11]. It appears only natural to assume that the features in the MCD spectrum observed in our case also originate from these transitions in the octahedral Fe^{3+} ions. The wavelengths of these features for the ferrite film are shifted by about 15 and 50 nm toward larger values (i.e., toward lower energies) compared with the iron borate, which can be attributed to a slightly smaller radius of the octahedral voids and the correspondingly higher crystal fields in the ferrite. The larger shift of the $^6A_{1g} \longrightarrow {}^4T_{2g}$ band compared with the $^6A_{1g} \longrightarrow {}^4E_g, {}^4A_{1g}$ band may be explained as due to the energy of the latter being weaker dependent on the crystal field (see, e.g., [13]). In this case, the weak overlapping positive features at ~500 and ~545 nm could be assigned to electronic transitions in the Fe^{3+} and Mn^{2+} ions residing in tetrahedral positions. The MCD due to ions in tetrahedra should be of a sign opposite to that produced by octahedral ions.

4. COMPULSIONS

Thus, solid-state reactions can be employed to advantage to synthesize films of both the magnetite and manganese ferrite solution and of the manganese ferrite from Mn and Fe bilayers deposited by thermal evaporation. The characteristic features of the FE spectra match with x-ray diffraction and Mössbauer effect data. We have succeeded in qualitatively relating the features in the MCD response with electronic transitions, primarily in trivalent iron ions, between crystal-field-split levels.

ACKNOWLEDGMENTS

We are grateful to G.N. Bondarenko for x-ray diffraction measurements.

This study was supported by the Russian Foundation for Basic Research (project no. 07-02-92174_NTsNI) and the Program "Development of the Scientific Potential of the Higher Education School."

REFERENCES

1. A. E. Sychev and A. G. Merzhanov, Usp. Khim. **73**, 157 (2004).
2. V. G. Miagkov and L. E. Bykova, Dokl. Akad. Nauk **354** (4–6), 777 (1997) [Dokl. Phys. Chem. **354** (4–6), 188 (1977)].
3. V. G. Miagkov, K. P. Polyakova, G. N. Bondarenko, and V. V. Polyakov, J. Magn. Magn. Mater. **258–259**, 358 (2003).
4. K. P. Polyakova, V. V. Polyakov, V. G. Miagkov, G. P. Solyanik, V. A. Seredkin, and O. I. Bachina, Phys. Met. Metallorg. **100** (Suppl. 1), S60 (2005).
5. S. N. Jasperson and S. E. Schnatterly, Rev. Sci. Instrum. **40**, 6761 (1969).
6. *Joint Committee on Powder Diffraction—International Centre for Diffraction Data, Database PDF-2*, No. 74-2403 (1997).
7. V. V. Chekin, *Mössbauer Spectroscopy of Iron, Gold, and Tin Alloys* (Énergoizdat, Moscow, 1981) [in Russian].
8. G. A. Sawatzky, Van Der Woude, and A. H. Morrish, Phys. Rev. **187**, 747 (1969).
9. Z. Šimša, P. Tailhades, L. Presmanes, and C. Bonningue, J. Magn. Magn. Mater. **242–245**, 381 (2002).
10. V. N. Zabluda, A. V. Malakhovskiĭ, and I. S. Édel'man, Fiz. Tverd. Tela (Leningrad) **27** (1), 133 (1985) [Sov. Phys. Solid State **27** (1), 77 (1985)].
11. A. V. Malakhovskiĭ, I. S. Édel'man, and V. N. Zabluda, Fiz. Tverd. Tela (Leningrad) **21** (7), 2164 (1979) [Sov. Phys. Solid State **21** (7), 1242 (1979)].
12. B. Kalska, J. J. Paggel, P. Fumagalli, J. Rybczynski, D. Satula, and M. Hilgendorff. J. Appl. Phys. **95**, 1343 (2004).
13. D. T. Sviridov, R. K. Sviridova, and Yu. F. Smirnov, *Optical Spectra of Transition Metal Ions in Crystals* (Nauka, Moscow, 1976) [in Russian].

Translated by G. Skrebtsov